Stabilization of a hopper with three reaction wheels

Igor Ryadchikov, Dmitry Sokolov, Andrei Biryuk, Semyon Sechenev,
Alexander Svidlov, Pavel Volkodav, Yury Mamelin, Kirill Popko, Evgeny
Nikulchev

HAL Id: hal-01927624
https://hal.inria.fr/hal-01927624

Submitted on 20 Nov 2018

Stabilization of a hopper with three reaction wheels

Igor Ryadchikov[a], Dmitry Sokolov[b], Andrei Biryuk[a], Semyon Sechenev[a], Alexander Svidlov[a], Pavel Volkodav[a], Yury Mamelin[a], Kirill Popko[a], and Evgeny Nikulchev[c]

[a] Kuban State University, 350040 Stavropolskaya, 149, Krasnodar, Russia

[b] UMR 7503, Université de Lorraine, CNRS, Vandœuvre-lès-Nancy, France

[c] Moscow Technological University (MIREA), 78 Vernadsky Avenue, Moscow 119454 Russia

Abstract

In this paper we present our ongoing hopping bot project. The hopper is stabilized with three reaction wheels; the main idea of the project is to develop a balancing system suitable for a dynamic stabilization of a bipedal walk for a non-anthropomorphic robot. We present an energy efficient hardware and software design of the stabilization system as well as a choice of electrical and mechanical parameters of the device.

1   Introduction

The idea of hopping bots is not new, we can cite Raibert's Hopper [5] that is stabilized by tilting its leg in two directions. Salto-1P jumper [7] is stabilized with a reaction lever in one direction and with two propellers for two others.

In contrast to these approaches we chose three reaction wheels because it allows to stabilize bigger (two-legged) robots. The difference with Cubli [2] or its follow-ups [1, 6] is the ability to move forward by hopping. It allows us to focus on the stabilization system and then to adapt the system for robots of different size and weight. Another novelty of this work is the mechatronic design of the reaction wheels aligned the body principal axes and sharing the same center of inertia. It leads to a better energetic efficiency of the stabilization system.

The context for the project is given by AnyWalker robotic chassis [3, 4] developed by our team (Figure 2, left). In its current state AnyWalker is able to walk using a static balance, it can climb stairs and walk over a complex terrain. We wish to improve walking abilities AnyWalker by introducing a dynamic stabilization.

Here we focus on the stabilization system only, therefore the bot is substantially simplified, it has one leg only and three reaction wheels. It allows us to remove from consideration complex disturbances like leg torsion/flexion or joint backlash (note that AnyWalker uses low-end servo drives).

Our bot will be able to advance with every hop by adding cyclic disturbances in the equilibrium attitude estimation, refer to the Figure 1 for an illustration. In these problem settings we can control the mechatronic system on the low level without generating trajectories or solving inverse kinematic problems. Direct control of the reaction wheels momenta allow us to avoid multi-layering in our software system thus effectively removing large delays and lag from the control loop.

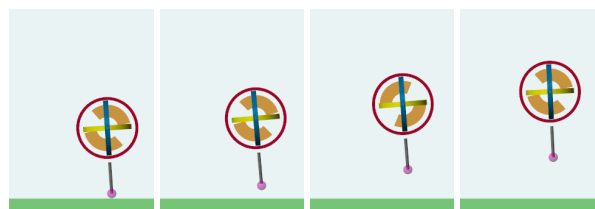The quality criterion used in this project is the energetic

Figure 1 One hop animation sequence. Note how the hopping allows the balancer to advance.
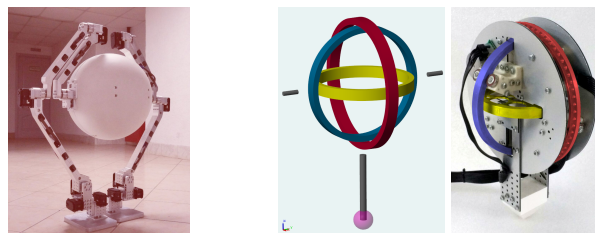
Figure 2 Left: AnyWalker robot developed by our team. Middle and right: hardware implementation of the self-balancing reaction wheels inverted pendulum.

efficiency of the dynamic stabilization. To achieve the goal we optimize for the electromechanical parameters given a hardware design choice, refer to the Figure 2. Please note that in its current state the hardware implementation does not have the hopping mechanism attached, thus serving as an inverted pendulum.

2   Theoretical background for the stabilization system

In what follows we use the notation:

- C is the moment of inertia of the pendulum without flywheels relative to its axis of symmetry.
- A is the moment of inertia of the pendulum without flywheels relative to any axis perpendicular to the symmetry axis passing through the pendulum support.
- A_w is the moment of inertia of the flywheel relative to any axis perpendicular to its axis of rotation and

passing through the point H.

- C_w is the moment of inertia of the flywheel relative to its axis of rotation.
- m is the mass of one flywheel.
- l is the distance from the fulcrum to the flywheel centers.
- b is the distance from the center of mass of the pendulum without flywheels to the fulcrum.
- M is the mass of a pendulum without flywheels.
- c_v is the back-emf ratio.
- c_u is the gain coefficient.
- g is the gravitational acceleration.
- ε is friction coefficient in the fulcrum.

2.1 Object dynamics equation

Hopper is a two-dimensional inverted pendulum. It is controlled by three reaction wheels. In our case, they all have a common center, see the Figure. We derive the differential equations of motion hopper by the method of Lagrangian mechanics.

2.1.1 Coordinate systems

All the coordinate systems used are the right-handed Cartesian coordinate systems. We will use the following coordinate systems: fixed with respect to the Earth and "frozen" into a pendulum. The origins of both the fixed and the "frozen" coordinate systems are at the pendulum support point, called O. The first axis of the fixed coordinate system is directed vertically upwards with respect to the Earth. The third axis of the "frozen" system is the axis of symmetry of the pendulum.

The position of the frozen system with respect to the fixed system will be determined using the Euler angles: ψ is the precession angle, θ is the nutation angle, φ is the intrinsic rotation angle. In what follows, we will be interested in the equilibrium point $\psi = \frac{\pi}{2}$, $\theta = \frac{\pi}{2}$, $\varphi = 0$, which corresponds to the vertical position of the third axis of the "frozen" in coordinate system.

We denote the basis of the fixed coordinate system by $\vec{i}_1, \vec{i}_2, \vec{i}_3$, and the basis of the "frozen" basis of the system by $\vec{e}_1, \vec{e}_2, \vec{e}_3$.

Let $\vec{\omega}$ be the angular velocity of rotation of the frozen system relative to the fixed one. Its expansion in the basis $\vec{e}_1, \vec{e}_2, \vec{e}_3$ has the form $\vec{\omega} = \omega_1 \vec{e}_1 + \omega_2 \vec{e}_2 + \omega_3 \vec{e}_3$, where

$$\omega_1 = \dot{\psi} \sin\theta \sin\varphi + \dot{\theta} \cos\varphi,$$

$$\omega_2 = \dot{\psi} \sin\theta \cos\varphi - \dot{\theta} \sin\varphi,$$

$$\omega_3 = \dot{\psi} \cos\theta + \dot{\varphi}.$$

2.1.2 The kinetic and the potential energy

We denote by T_0 the kinetic energy of the pendulum without the kinetic energy of the flywheels. It is known that

$$T_0 = \frac{1}{2} \vec{\omega} \cdot \mathscr{J}(\vec{\omega}),$$

where $\mathscr{J}$ is the inertia operator of a pendulum without flywheels. In the "frozen" coordinate system, it has the

following matrix $J = \mathrm{diag}(A, A, C)$. Here A and C are constants (parameters of the pendulum). We have

$$T_0 = \frac{1}{2} A(\omega_1^2 + \omega_2^2) + \frac{1}{2} C \omega_3^2.$$

Consider a flywheel whose axis of rotation is parallel to the vector $\vec{e}_k$. We call it k-th flywheel. Its kinetic energy is denoted T_k, and its inertia operator with respect to point of H will is denoted by $\mathscr{J}_k$.

By König's decomposition theorem we have

$$T_k = \frac{1}{2} (\vec{\omega} + \dot{\alpha}_k \vec{e}_k) \cdot \mathscr{J}_k (\vec{\omega} + \dot{\alpha}_k \vec{e}_k) + \frac{1}{2} m \vec{v}_H^2,$$

where $\dot{\alpha}_k$ is the rotation speed of the k-th flywheel relative to the body of the inverted pendulum.

Consider a coordinate system with the origin at the point H, whose axes are are parallel to the basis $\vec{e}_1, \vec{e}_2, \vec{e}_3$. In this system, the matrices of the operators $\mathscr{J}_k, k = \overline{1,3}$ have the following form:

$$J_1 = \mathrm{diag}(C_w, A_w, A_w),$$
$$J_2 = \mathrm{diag}(A_w, C_w, A_w),$$
$$J_3 = \mathrm{diag}(A_w, A_w, C_w),$$

where A_w, C_w are the flywheel parameters. Let l be the length of OH. Taking into account $\vec{v}_H = \vec{\omega} \times OH = \vec{\omega} \times l\vec{e}_3$, we obtain

$$T_k = \frac{1}{2} (\vec{\omega} + \dot{\alpha}_k \vec{e}_k) \cdot \mathscr{J}_k (\vec{\omega} + \dot{\alpha}_k \vec{e}_k) + \frac{1}{2} m l^2 (\vec{\omega} \times \vec{e}_3)^2.$$

The total kinetic energy of the pendulum with flywheels

$$T = \sum_{k=0}^{3} T_k = T_0 + \frac{3}{2} m l^2 (\vec{\omega} \times \vec{e}_3)^2 +$$

$$\sum_{k=1}^{3} \frac{1}{2} (\vec{\omega} + \dot{\alpha}_k \vec{e}_k) \cdot \mathscr{J}_k (\vec{\omega} + \dot{\alpha}_k \vec{e}_k) =$$

$$= \left(\frac{1}{2} A + \frac{3}{2} m l^2 + A_w + \frac{1}{2} C_w \right) (\omega_1^2 + \omega_2^2) +$$

$$\left(\frac{1}{2} C + A_w + \frac{1}{2} C_w \right) \omega_3^2 + \frac{1}{2} C_w \sum_{k=1}^{3} \dot{\alpha}_k^2 + C_w \sum_{k=1}^{3} \dot{\alpha}_k \omega_k.$$

The total potential energy is given by the following expression

$$\Pi = (3ml + bM) g \sin\psi \sin\theta = Y \sin\psi \sin\theta,$$

where

$$Y = (3ml + bM) g.$$

2.1.3 Generalized forces

We introduce generalized coordinates: $q_1 = \psi - \pi/2$, $q_2 = \theta - \pi/2$, $q_3 = \varphi$, $q_4 = \alpha_1$, $q_5 = \alpha_2$, $q_6 = \alpha_3$. We denote the corresponding generalized forces: Q_1, Q_2, Q_3, Q_4, Q_5, Q_6.

Let $\vec{M}_k$ be the moment developed by the engine of k-th flywheel. We have $\vec{M}_k = M_k \vec{e}_k$. We use the following model for flywheels engines $M_k = c_u u_k - c_v \dot{\alpha}_k$, $k =$

1, 2, 3. Thus, the active moment of force $\vec{M}_k$ will act on the k-th flywheel, The moment of force that act on the pendulum is as follows:

$$\vec{M}_0 = \vec{M}_{\text{fr}} - \vec{M}_1 - \vec{M}_2 - \vec{M}_3,$$

where $\vec{M}_{\text{fr}} = \varepsilon\vec{\omega}$, ε is a negative constant.

Then the generalized forces are as follows: $Q_1 = \varepsilon(\dot{q}_1 - \dot{q}_3\sin q_2)$, $Q_2 = \varepsilon\dot{q}_2$, $Q_3 = \varepsilon(\dot{q}_3 - \dot{q}_1\sin q_2)$, $Q_4 = M_1$, $Q_5 = M_2$, $Q_6 = M_3$.

2.1.4 Lagrange equations of the second kind

The Lagrangian L is defined by the formula $L = T - \Pi$. Lagrange equations of the second kind have the form

$$\frac{d}{dt}\left(\frac{\partial L}{\partial \dot{q}_i}\right) - \frac{\partial L}{\partial q_i} = Q_i, \quad i = 1,\ldots,6.$$

Performing elementary calculations and substituting expressions for all partial derivatives, we obtain these equations in an explicit form. Transforming to the normal form, we obtain the following expressions:

$$\ddot{q}_k = G_k, \quad k = 1,\ldots,6,$$

where

$$G_1 = -\frac{1}{2P\cos^2 q_2}\left(F_1 + F_3\sin q_2\right), \quad G_2 = -\frac{1}{2P}F_2,$$

$$G_3 = -\frac{1}{2P_3}\left(F_1\frac{P_3\sin q_2}{P\cos^2 q_2} + F_3\left(1 + \frac{P_3\sin^2 q_2}{P\cos^2 q_2}\right)\right),$$

$$G_k = \frac{M_{k-3}}{C_{\text{w}}} - \sum_{j=1}^{3}\frac{\partial\omega_{k-3}}{\partial q_j}\dot{q}_j - \sum_{j=1}^{3}\frac{\partial\omega_{k-3}}{\partial\dot{q}_j}G_j, k = 4,5,6.$$

$$F_i = \sum_{k=1}^{3}\frac{\partial^2 W}{\partial\dot{q}_i\partial q_k}\dot{q}_k + \frac{\partial W}{\partial q_i} + C_{\text{w}}\sum_{k=1}^{3}\dot\alpha_k\frac{\partial\omega_k}{\partial q_i} - \frac{\partial\Pi}{\partial q_i} - Q_i +$$

$$C_{\text{w}}\left(\sum_{k=1}^{3}\left(\frac{M_k}{C_{\text{w}}} - \sum_{j=1}^{3}\frac{\partial\omega_k}{\partial q_j}\dot{q}_j\right)\frac{\partial\omega_k}{\partial\dot{q}_i} + \sum_{k=1}^{3}\dot\alpha_k\sum_{j=1}^{3}\frac{\partial^2\omega_k}{\partial\dot{q}_i\partial q_j}\dot{q}_j\right),$$

$$i = 1,2,3, \quad P = \tfrac{1}{2}A + \tfrac{3}{2}ml^2 + A_{\text{w}}, P_3 = \tfrac{1}{2}C + A_{\text{w}},$$

$$W = \left(P + \frac{1}{2}C_{\text{w}}\right)\left(\omega_1^2 + \omega_2^2\right) + \left(P_3 + \frac{1}{2}C_{\text{w}}\right)\omega_3^2.$$

2.2 Linearized equations of dynamics

Linearizing the equations of motion in the neighborhood of the point $q_i = \dot{q}_i = 0$, $i = 1,\ldots,6$, $u_k = 0$, $k = 1,2,3$, we obtain the following equations:

$$\ddot{q}_1 = \frac{1}{2P}\left(Yq_1 + \varepsilon\dot{q}_1 + M_2\right), \tag{1}$$

$$\ddot{q}_2 = \frac{1}{2P}\left(Yq_2 + \varepsilon\dot{q}_2 + M_1\right), \tag{2}$$

$$\ddot{q}_3 = \frac{1}{2P_3}\left(\varepsilon\dot{q}_3 + M_3\right), \tag{3}$$

$$\ddot\alpha_1 = -\frac{Yq_2 + \varepsilon\dot{q}_2}{2P} + \left(\frac{1}{C_{\text{w}}} + \frac{1}{2P}\right)M_1,$$

$$\ddot\alpha_2 = -\frac{Yq_1 + \varepsilon\dot{q}_1}{2P} + \left(\frac{1}{C_{\text{w}}} + \frac{1}{2P}\right)M_2,$$

$$\ddot\alpha_3 = -\frac{\varepsilon\dot{q}_3}{2P_3} + \left(\frac{1}{C_{\text{w}}} + \frac{1}{2P_3}\right)M_3.$$

Similarly, we can write Lagrange equations of the second kind for the "Cubli" arrangement of flywheels, in which the geometric position of the flywheels is given by the orthogonal transformation with the matrix

$$B = \begin{pmatrix} \sqrt{\frac{2}{3}} & 0 & -\sqrt{\frac{1}{3}} \\ -\sqrt{\frac{1}{6}} & \sqrt{\frac{1}{2}} & -\sqrt{\frac{1}{3}} \\ -\sqrt{\frac{1}{6}} & -\sqrt{\frac{1}{2}} & -\sqrt{\frac{1}{3}} \end{pmatrix}$$

in basis $\vec{e}_1$, $\vec{e}_2$, $\vec{e}_3$. In this case the linearization of the Lagrange equations has the following form:

$$\ddot{q}_1 = \frac{Yq_1 + \varepsilon\dot{q}_1}{2P} - \frac{M_2 - M_3}{2\sqrt{2}P},$$

$$\ddot{q}_2 = \frac{Yq_2 + \varepsilon\dot{q}_2}{2P} - \frac{2M_1 - M_2 - M_3}{2P\sqrt{6}},$$

$$\ddot{q}_3 = \frac{\varepsilon\dot{q}_3}{2P_3} + \frac{M_1 + M_2 - M_3}{2P_3\sqrt{3}},$$

$$\ddot\alpha_1 = -\frac{Yq_2 + \varepsilon\dot{q}_2}{P\sqrt{6}} + \frac{\varepsilon\dot{q}_3}{2P_3\sqrt{3}} +$$

$$\left(\frac{1}{C_{\text{w}}} + \frac{1}{3P} + \frac{1}{6P_3}\right)M_1 + \frac{P - P_3}{6PP_3}M_2 - \frac{P + P_3}{6PP_3}M_3,$$

$$\ddot\alpha_2 = -\frac{Yq_1 + \varepsilon\dot{q}_1}{2P\sqrt{2}} + \frac{Yq_2 + \varepsilon\dot{q}_2}{2P\sqrt{6}} + \frac{\varepsilon\dot{q}_3}{2P_3\sqrt{3}} +$$

$$\frac{P - P_3}{6PP_3}M_1 + \left(\frac{1}{C_{\text{w}}} + \frac{1}{3P} + \frac{1}{6P_3}\right)M_2 - \frac{P + P_3}{6PP_3}M_3,$$

$$\ddot\alpha_3 = \frac{Yq_1 + \varepsilon\dot{q}_1}{2P\sqrt{2}} + \frac{Yq_2 + \varepsilon\dot{q}_2}{2P\sqrt{6}} - \frac{\varepsilon\dot{q}_3}{2P_3\sqrt{3}} -$$

$$\frac{P + P_3}{6PP_3}M_1 - \frac{P + P_3}{6PP_3}M_2 + \left(\frac{1}{C_{\text{w}}} + \frac{1}{3P} + \frac{1}{6P_3}\right)M_3.$$

2.3 Synthesis of the control

The control u_1, u_2, u_3 of flywheel motors is selected by the LQR method, while the functional is minimized:

$$J = \int_0^\infty \sum_{i=1}^{2} q_i^2\,dt + \int_0^\infty \sum_{i=1}^{3}(u_i^2 + \dot{q}_i^2 + \dot\alpha_i^2)\,dt.$$

This procedure is carried out both for our case and for the case of the flywheels à la Cubli.

2.4 Energy consumption comparison

While conducting numerical experiments we have used the following values of the electromechanical parameters of the inverted pendulum : $m = 0.2 kg$; $l = 0.085 m$; $b = 0.08 m$; $M = 0.4 kg$; $c_v = 5 \cdot 10^{-5} N \cdot m \cdot s$; $c_u = 0.025 N \cdot m/V$; $A_w = 2.85 \cdot 10^{-4} kg \cdot m^2$; $C_w = 5.7 \cdot 10^{-4} kg \cdot m^2$; $A = 1.6 \cdot 10^{-3} kg \cdot m^2$; $C = 1.52 \cdot 10^{-3} kg \cdot m^2$; $g = 9.81 m/s^2$; $\varepsilon = -0.001 N \cdot m \cdot s$.

We conducted a series of numerical experiments for the inverted pendulum to estimate the energy costs required for elimination of various initial disturbances. In this article we present the results of only a few of them. The results of others are similar.

The table shows the energy costs for Cubli-like and our flywheel arrangement geometry (the last two columns) for the indicated values of the initial perturbations for the variables q_1, q_2, $\dot{q}_1$, $\dot{q}_2$. The initial perturbations for the remaining variables $q_3, \dot{q}_3, \dot{\alpha}_1, \dot{\alpha}_2, \dot{\alpha}_3$ were set to zero for those five experiments.

N	q_1	q_2	$\dot{q}_1$	$\dot{q}_2$	E_c	E_o
1	0.1	0	0	0	13.1	10.9
2	0	0.1	0	0	11.6	10.9
3	0.1	0.1	0	0	27.1	21.8
4	0	0	0.1	0	0.184	0.156
5	0	0	0	0.1	0.165	0.156

Here $E_c = \int_0^\infty \sum_{i=1}^{3} |u_i \dot{\alpha}_i| dt$ is the energy cost of the Cubli-like stabilization system, and $E_o = \int_0^\infty \sum_{i=1}^{3} |u_i \dot{\alpha}_i| dt$ is the energy cost of our stabilization system. The experimental data show that our flywheel arrangement is more energy-efficient.

As for the optimization for the mechanical parameters of the flywheels, it is easy to see that in our case the equations of motion (1)–(3) are independent one from another. We can therefore optimize the flywheel parameters in simple 1D inverted pendulum settings. Given flywheel parameters, we can find maximum initial angle such that we can stabilize the pendulum with input constraints. Then we vary the parameters to maximize this angle.

3 Experimental study

Figure 2 shows the hardware implementation of the 2D inverted pendulum. We used STM32F407 as a main controller, it queries IMU6050-based accelerometers/gyroscopes via an i2c bus and filters the data via Madgwick sensor fusion algorithm. Reaction wheels are controlled with Maxon EPOS2 50/5 torque amplifier, three Maxon EC45-flat motors are used to drive the wheels. Figure 3 shows a stabilization example starting from initial inclination $q_1 = q_2 = 0.1$.

We conducted a series of numerical experiments to see if we achieve a stabilization of a hopping bot and we witness an asymptotically stable behavior with simple linear regulators. One hop animation sequence is shown in Figure 1.
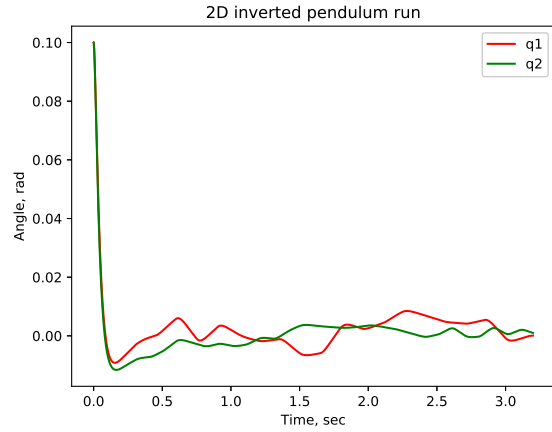

Figure 3 Stabilization of our hardware implementation of the 2D inverted pendulum.

4 Conclusion

To conclude, we propose a hardware design and corresponding theoretical basis for building robots stabilized with three reaction wheels. The hopper we propose here can be built at a fraction of cost of a bigger walking robot, while maintaining the complexity of the control, thus making it well suitable for the control education process.

5 Literature

[1] Johannes Mayr, Franz Spanlang, and Hubert Gattringer. Mechatronic design of a self-balancing three-dimensional inertia wheel pendulum. *Mechatronics*, 30:1 – 10, 2015.

[2] M. Muehlebach and R. D'Andrea. Nonlinear analysis and control of a reaction-wheel-based 3-d inverted pendulum. *IEEE Transactions on Control Systems Technology*, 25(1):235–246, Jan 2017.

[3] I. Ryadchikov, S. Sechenev, S. Sinitsa, A. Svidlov, P. Volkodav, A. Feshin, A. Alotaki, A. Bolshakov, M. Drobotenko, and E. Nikulchev. Design and control of self-stabilizing angular robotics anywalker. *International Journal of Advanced Computer Science and Applications*, 8:29–34, 10 2017.

[4] I. Ryadchikov, S. Sechenev, A. Svidlov, S. Sinitsa, and E. Nikulchev. Development of a self-stabilizing robotic chassis for industry. *MATEC Web of Conferences*, 99:02007, 01 2017.

[5] Seshashayee S. Murthy and Marc H. Raibert. 3d balance in legged locomotion: modeling and simulation for the one-legged case. *ACM SIGGRAPH Computer Graphics*, 18:27–27, 1984.

[6] Abdullah Türkmen, Yusuf Korkut, Mustafa Erdem, Ömer Gönül, and Volkan Sezer. Design, implementation and control of dual axis self balancing inverted pendulum using reaction wheels. *ELECO 2017*.

[7] Duncan W. Haldane, Justin K. Yim, and Ronald S. Fearing. Repetitive extreme-acceleration (14-g) spatial jumping with salto-1p. *2017 IEEE/RSJ International Conference on Intelligent Robots and Systems*.